



HAL
open science

Low Phase Noise Direct-Modulation Optoelectronic Oscillator

Brian Siquin, Marco Romanelli, Steve Bouhier, Ludovic Frein, Mehdi Alouini, Marc Vallet

► **To cite this version:**

Brian Siquin, Marco Romanelli, Steve Bouhier, Ludovic Frein, Mehdi Alouini, et al.. Low Phase Noise Direct-Modulation Optoelectronic Oscillator. *Journal of Lightwave Technology*, 2021, 39 (24), pp.7788-7793. 10.1109/jlt.2021.3111703 . hal-03487897

HAL Id: hal-03487897

<https://hal.science/hal-03487897>

Submitted on 17 Dec 2021

HAL is a multi-disciplinary open access archive for the deposit and dissemination of scientific research documents, whether they are published or not. The documents may come from teaching and research institutions in France or abroad, or from public or private research centers.

L'archive ouverte pluridisciplinaire **HAL**, est destinée au dépôt et à la diffusion de documents scientifiques de niveau recherche, publiés ou non, émanant des établissements d'enseignement et de recherche français ou étrangers, des laboratoires publics ou privés.

Low Phase Noise Direct-Modulation Optoelectronic Oscillator

BRIAN SINQUIN, MARCO ROMANELLI, STEVE BOUHIER,
LUDOVIC FREIN, MEHDI ALOUINI, MARC VALLET

Institut FOTON, UMR 6082, Univ. Rennes1

brian.sinquin@univ-rennes1.fr

September 13, 2021

Abstract

A direct-modulation OEO (DM-OEO) generating stable 10 GHz and 20 GHz signals is presented. A single loop and a dual loop approach are implemented and compared. We show an output signal of 15 dBm RF power, and a phase noise as low as -135 dBc/Hz at 10 kHz offset from the 10 GHz carrier. The 20 GHz second harmonic exhibits a noise level of -127 dBc/Hz at 10 kHz. A high spur level reduction is also obtained in the dual loop architecture.

I. INTRODUCTION

The generation of pure microwave signals with low phase noise is a requirement for applications as diverse as coherent telecommunications, clock sharing, or tele-detection. Methods based on quartz oscillators and frequency multiplication for generating high frequency carriers are not sufficient for current needs, and a new generation scheme called Opto-Electronic Oscillator (OEO) was introduced in the late 90's to lower the phase noise at high carrier frequencies (typically a few tens of GHz) [1]. This system is based on the insertion of a low loss (0.2 dB/km) km-long optical fiber in an opto-RF feedback loop. The optical part of the loop serves as a long delay line, resulting in a high-Q resonator for the optically-carried RF signal. Most of the OEO architectures include a Mach-Zehnder Modulator (MZM) as an external optical intensity modulation element [2]. An alternative to this widespread scheme is direct modulation (DM) of the injection current of a semiconductor laser. DM is arguably the simplest possible OEO scheme [3], and offers a cheaper and more compact approach. In comparison with the huge literature on the classical MZM-based architecture, the DM approach has been much less explored. An early paper studying the effect of delayed feedback on the laser current is [4]. At that time people were strongly interested in instabilities, however the authors already

noted that such a system “may be conveniently used as a high frequency source”. Many subsequent studies on semiconductor lasers with optoelectronic feedback were indeed focused on dynamical instabilities [2]. More recently, some authors proposed setups based on various combinations of optoelectronic feedback and optical injection [5] or feedback [6], [7] with the aim of generating stable and possibly tunable microwave signals. Direct current modulation of a microsquare laser was used in [8] to generate tunable signals with good phase noise. Very recently, an architecture similar to the one presented here was published [9], showing OEO operation between 8 and 12 GHz.

In this paper, we implement the DM-OEO scheme in its simplest form, and study in detail its performances as a generator of high frequency signals. In addition to the single-loop architecture, we study a dual-loop scheme which improves some figures of the OEO, at the expense of an increased complexity. Our system exhibits stable single-frequency oscillation of a 10 GHz carrier, with 15 dBm output RF power and -135 dBc/Hz phase noise at 10 kHz offset from the carrier. The rejection ratio of adjacent resonant modes is 60 dB in the single-loop scheme, and more than 80 dB with the dual loop. Furthermore, due to nonlinearities in the feedback loop, 20 GHz output is also available. These results constitute, to the best of our

knowledge, the state-of-the-art of DM-OEOs, and show that the performances of DM-OEOs are comparable to standard OEOs. Thus, direct modulation is a valuable alternative, which should be considered in particular when one aims at monolithic photonic chips [10]. The paper is organized as follows. In section II we present the experimental results of the single and dual loop DM-OEO, together with a comparison to a simple phase noise model. We offer some conclusions and perspectives in section III.

II. EXPERIMENTAL RESULTS

II.1. Single loop DM-OEO

The simplest possible OEO consists in a directly-modulated laser, controlled by a bias current and a modulation current (Fig. 1). Light from the laser passes through a km-long optical fiber before being detected by a photodiode. The generated photocurrent is then filtered by a high-Q dielectric resonant filter centered at 10 GHz, suitably amplified, and fed back into the laser modulation port. In the standard OEO [1], the MZM provides the optical modulation function. Thanks to its nonlinear response, the MZM also displays a power saturation behavior that sets the stable working point of the oscillator, fulfilling the Barkhausen condition $\|A\beta(f_0)\| = 1$, where A and $\beta(f_0)$ represent the gain and the transfer function of the feedback loop respectively [11]. In our scheme, it is the electrical amplifier that plays the role of the saturating component, stabilizing the circulating RF power.

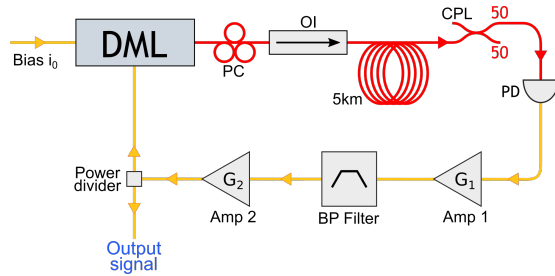


Figure 1: Single loop DM-OEO scheme. *DML*: Directly Modulated Laser, *OI*: Optical isolator, *PC*: Polarization controller *CPL*: Optical 50/50 coupler, *PD*: Photodiode.

Fig. 1 shows the experimental setup of the single loop DM-OEO architecture. A commercial telecommu-

nication DFB laser (NEL, NLK5C5E2KA), with a modulation bandwidth larger than 10 GHz and an overall efficiency $\eta_L = 0.07$ W/A is used as the electrical to optical conversion component at 10 GHz. The optical delay is induced by a 5 km-long SMF fiber, which is connected to a 50/50 coupler offering at the same time an optical output port to the DM-OEO and an adapted level of optical power on the photodiode. The photodiode is an InGaAs semiconductor PIN photo-diode (Nortel, PP-10G) with a responsivity $\eta_{Ph.D} = 0.88$ A/W, a saturation power of 0 dBm and a 500 V/A transimpedance gain at its output. The output voltage is amplified by a 36 dB RF amplifier (Amp 1) with a +14 dBm P1dB output power and a 0.7 dB typical noise figure. A custom high Q-factor ($Q = 2500$) dielectric filter from LAAS¹ with a -3 dB bandwidth of 4 MHz and centered around $f_0 = 10.00485$ GHz is added at the output of Amp 1. Due to some degradation of its internal connectors, the filter displays insertion losses of about 10 dB. The filtered signal is then amplified again by a 28 dB RF amplifier (Amp 2) which has a P1dB output power of 18 dBm and a 8 dB typical noise figure. After Amp 2, the signal passes through a 3 dB power divider. Half of the RF power is fed back to the laser through the RF input port, the other half constitutes the useful output signal, and is directed towards a phase noise analyzer (Rohde & Schwarz FSWP26). The laser is driven by a continuous bias current i_0 , and controlled in temperature. In our experiment we set the bias current i_0 at 70 mA (the laser threshold is $i_{th} = 10$ mA) and measure a mean optical power of 4.6 mW at the output of the laser and 1.35 mW at the input of the photodiode. An optical isolation stage was also added in front of the optical fiber in order to avoid optical feedback in the laser and the dynamical instabilities that it could cause.

Fig. 2 shows the RF spectrum of the output signal from the DM-OEO. An extracted electrical power of 15 dBm is available at the carrier frequency of 10.00436 GHz. The adjacent peaks are non-oscillating resonant modes of the delay loop, apart from each other by the Free Spectral Range $FSR = \frac{c}{nL} = 40$ kHz, where n and L are the fiber refractive index and length respectively. The rejection ratio of the highest peaks is of 60 dB.

The spectrum profile presented in Fig. 2 is stable in time, in the sense that no mode hops are observed.

¹Laboratoire d'Analyse et d'Architecture des Systèmes F-31077 Toulouse, France

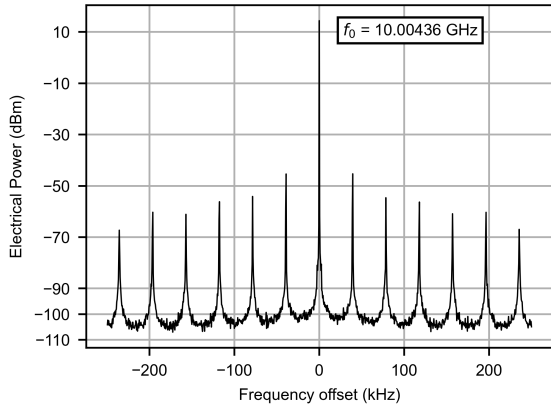


Figure 2: Electrical spectrum of the 10 GHz carrier in the single loop DM-OEO. Span: 500 kHz. Resolution Bandwidth: 10 Hz.

However, a slow constant drift of the carrier frequency is present. We quantified the frequency drift by configuring the ESA trace settings on Max Hold (Fig. 3). We observed a drift towards low frequencies of 1 kHz

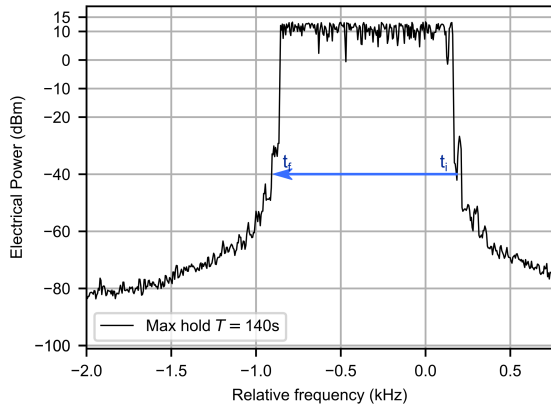


Figure 3: Max hold of the 10 GHz carrier drift in the single loop DM-OEO. Resolution Bandwidth: 5 Hz. Measurement time: 140s. Center frequency: 10.004355 GHz.

in 140s, corresponding to 7.2 Hz/s. This absolute frequency stability is obtained without any particular thermal or mechanical stabilization effort (the setup is inside a non-thermalized plexiglass box, on an optical table). One may expect that such a drift would eventually lead to a mode hop. However, a drift of the order of the FSR would require more than one hour, consistent with our observation of no mode hops over a 10

minutes time scale. Given the fact that the carrier frequency diminishes in time, the drift may be attributed to a slow thermal expansion of the fiber loop.

The distortions of the saturated second amplifier also generate harmonics at higher frequencies. Our ESA cannot analyze frequencies beyond 26.5 GHz so we can only observe the second harmonic carrier (at 20 GHz). Such a behavior has already been used to create a third harmonic generator in an OEO[12].

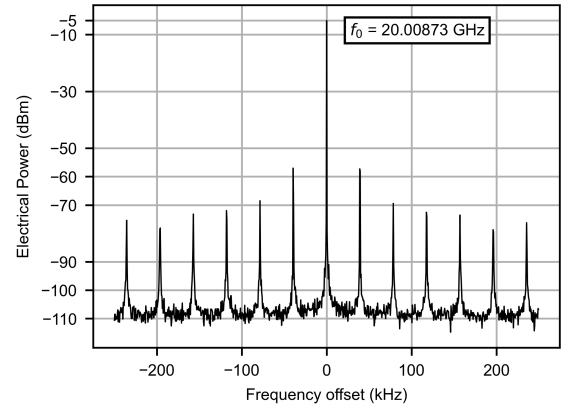


Figure 4: Electrical spectrum of the 20 GHz carrier in the single loop DM-OEO. Span: 500 kHz. Resolution Bandwidth: 30 Hz. The difference in resolution bandwidth with respect to Fig. 2 is inessential and does not impact the spectrum.

Fig. 4 shows the RF spectrum of the 2nd harmonic, exhibiting an oscillation power of -5 dBm and a rejection ratio of 50 dB of the non-oscillating modes.

In Fig. 5 we present the phase noise spectra of both 10 GHz and 20 GHz signals, measured with Rohde & Schwarz FSWP26 allowing the tracking of the oscillating frequency and measurement of precise phase noise spectra using cross correlation to lower the influence of its internal oscillator noise. Our experiment shows a phase noise of -135 dBc/Hz at 10 kHz offset from the 10 GHz carrier and of -127 dBc/Hz at 10 kHz offset from the 20 GHz carrier. The phase noise floors are of -140 dBc/Hz at 10 GHz and -130 dBc/Hz at 20 GHz respectively. The non-oscillating modes appear as spurs in the phase noise spectra. The highest ones are at 40 kHz from the carriers, and their noise level is between -60 dBc/Hz and -80 dBc/Hz (actually the spurs levels suggested by Fig. 5 are probably underestimated by about 10 dB, see the discussion in II.3). For the sake of

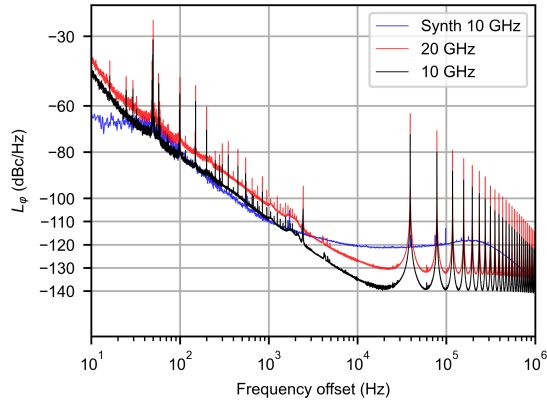


Figure 5: Phase noise spectrum of the 10 GHz & 20 GHz carriers in the single loop DM-OEO. Synth: Phase noise of a low-noise Rohde & Schwarz SMF100A-B1 OCXO electrical synthesizer at 10 GHz. Measurements were made with a 50 XCORR factor (50 cross correlations at 10 Hz) and a 0.1% RBW.

comparison, we plotted the phase noise of a electrical low-noise synthesizer (Rohde & Schwarz SMF100A-B1 OCXO) oscillating at 10 GHz. One can see that the DM-OEO signal is as good as the synthesizer between 30 Hz and 2 kHz, and better than it after 2 kHz, apart from the spurs. For instance, at 10 kHz from the carrier the OEO phase noise is 15 dB below the synthesizer.

II.2. Dual loop DM-OEO

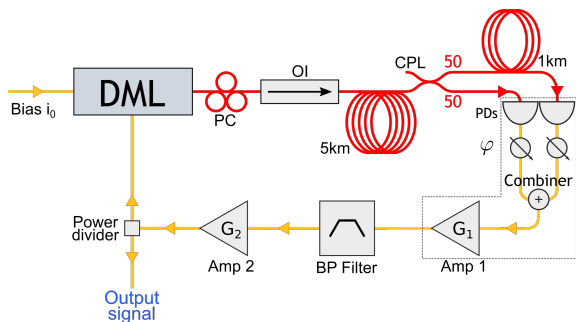


Figure 6: Dual loop DM-OEO schematic. **DML:** Directly Modulated Laser, **PC:** Polarization controller, **OI:** Optical isolator, **CPL:** Optical 50/50 coupler, **PDs:** Photo-diodes, φ : Phase-shifters.

The single loop OEO architecture provides a high

rejection ratio and low phase noise, but non-resonant spurs degrade the phase noise at the optical FSR frequencies and they can be very high (-60 dBc/Hz or more). One way to lower them is to use a dual loop approach [13]. Such an approach is not specific to the DM-OEO, and has been widely studied with external modulation schemes. By splitting the laser output signal in two different paths with different delays and combining them electrically after the photodiode detection, we are able to filter out the spurs by RF interferometry.

Fig. 6 shows our experimental implementation of the dual loop DM-OEO. At variance with the single loop scheme, the second output port of the 50/50 coupler is connected to a 1 km fiber followed by a second identical PP-10G transimpedance photodiode. Then each of the two electrical signals passes through a variable phase shifter before being combined. The resulting signal is amplified by the 36 dB amplifier and the following link scheme is the same as that of the previous section. Our configuration corresponds to a dual loop architecture with 5 km and 6 km loop lengths. Only the modes that are resonant for both loops are not filtered out, and thus are modes of the overall oscillator. We optimized the phase noise by setting the bias current of the laser to 73 mA. We then measured a laser optical power of 4.9 mW, an optical power of 1.2 mW at the end of the 1km fiber and 1.3 mW on the second output port of the coupler. Empirically we observed that the bias current, the laser modulation power, and the electrical phase-shifts are determinant in the optimization of the phase noise level. We also observed, consistently with [14], that the performance in terms of phase noise is improved by adjusting the optical power slightly beyond the saturation level of the photodiodes. Indeed, the P1dB input power of our detector is 1 mW but the mean optical power we inject is around 1.2 mW.

The resulting electrical spectrum at 10 GHz (Fig. 7) exhibits a high rejection ratio of more than 80 dB. In particular, the closest-to-the-carrier spurs (at 40 kHz) are at -90 dBm for a carrier power of 13 dBm. As we use the second RF amplifier (28 dB) at its saturation point, we observe SHG at 20 GHz as in the single loop architecture, with a relatively high -7 dBm power at 20 GHz, and a high rejection ratio of 90 dB near the carrier. The dual loop architecture exhibits better RF spectra profiles, while the signal powers remain of the

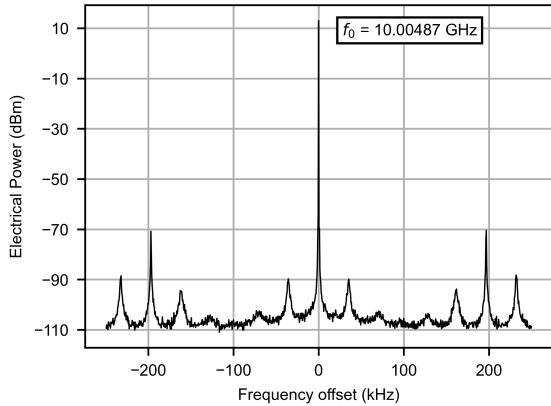


Figure 7: Electrical spectrum of the 10 GHz carrier in the dual loop DM-OEO. Span: 500 kHz. Resolution Bandwidth: 5 Hz.

same order both at 10 and 20 GHz.

Fig. 8 shows the phase noise of the two carriers in the dual loop setup. The phase noise floors are similar to those of the single loop architecture (-140 dBc/Hz for the 10 GHz carrier), but they can dive off by 5 dB at certain frequencies. For example, the 10 GHz carrier phase noise floor can reach a value of -145 dBc/Hz. This indicates that the real floor should be at -145 dBc/Hz but that the electrical interference quality (the contrast) is degrading the phase noise level.

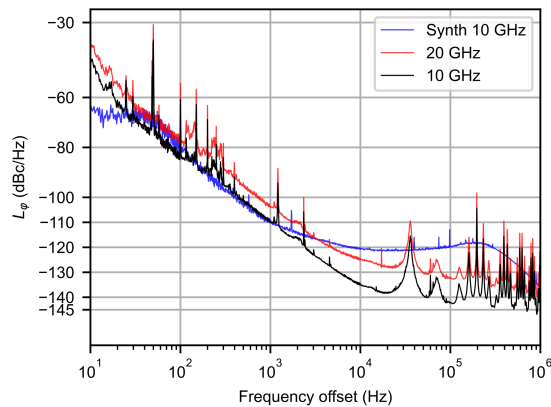


Figure 8: Phase noise spectrum of the 10 GHz & 20 GHz carriers in the dual loop DM-OEO. Synth: Phase noise of a low-noise Rohde & Schwarz SMF100A-B1 OCXO electrical synthesizer at 10 GHz. Measurements were made with a 30 XCORR factor (30 cross correlations at 10 Hz) and a 1% RBW.

The most notable phase noise difference is the level of the spurs that has been highly improved. The first spur of the 10 GHz carrier has a phase noise of -115 dBc/Hz at 40 kHz offset. This is at least 43 dB less than in the single loop configuration. Moreover, because of the periodicity of the Vernier effect we still observe high spurs but less frequently. The highest spur is at 195 kHz from the 10 GHz carrier with a phase noise level of about -100 dBc/Hz. We used the same method than in the previous section to measure the drift of the 10 GHz carrier. The dual loop DM-OEO shows a drift velocity of 9.2 Hz/s towards low frequencies.

II.3. Comparison with a phase noise model

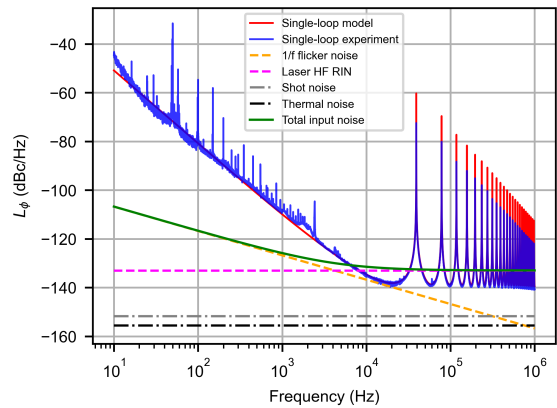


Figure 9: Comparison of the model eq. 1 with the experimental results. The input noises (thermal, shot, laser RIN, flicker) as well as the resulting total input noise are also shown.

In order to obtain some insights in the performances of our DM-OEO, we compared our experimental results with a simplified version of the model proposed by Lelièvre et al. [15], using their proposed eq. (3):

$$S_{\phi_{osc}}(f) = \left| \frac{\beta_f(f)}{1 - \beta_f(f)\beta_d(f)} \right|^2 S_{\psi_1}(f) \quad (1)$$

where $S_{\phi_{osc}}(f)$ is the phase noise spectrum of the OEO, $\beta_f(f)$ and $\beta_d(f)$ the microwave filter and the delay line transfer functions respectively, and $S_{\psi_1}(f)$ the input phase noise after the photodiode.

We considered the following input noise sources: thermal and shot noise, laser relative intensity noise (RIN) at the oscillation frequency f_0 , and a flicker noise source with spectral density of the form $b_{-1}f^{-1}$. So the input phase noise $S_{\psi_1}(f)$ reads

$$S_{\psi_1}(f) = S_{th} + S_{shot} + S_{RIN_{HF}} + S_{flicker} \quad (2)$$

The laser RIN at 10 GHz was experimentally measured to be -137 dB/Hz. We calculated the corresponding input phase noise using Lelièvre's formulas (12) et (13), with a modulation depth $m = 0.9$, and injected it in eq. 1. As Fig. 9 shows, there is a very good agreement with the experimental noise floor (note that the minima of the phase noise of the oscillator are 6 dB below the in-loop noise level, an effect discussed in [11], p. 139). So we can conclude that, for frequencies above 10 kHz, the laser RIN at high frequency is the factor limiting the performances of our system. In order to reproduce the experimental noise spectrum for frequencies below 10 kHz, it is necessary to include an additional noise source $S_{flicker} = b_{-1}f^{-1}$ with $b_{-1} = 2.1 \cdot 10^{-10}$. This additional flicker noise allows obtaining a good agreement with experiments, and is most probably due to the RF amplifiers and to the conversion of laser frequency noise (to which frequency chirping caused by direct modulation may also contribute) into RF phase noise via the fiber dispersion. At present the data for these two contributions are not available to us, and we cannot say which of the two effects is the most important. In fig. 9, the level of the spurs is higher in the model than in the experimental curve. This is probably not a limitation of the model, but an artifact due to the insufficient frequency resolution of the phase noise measurement, as in [15]. This interpretation is corroborated by Fig. 10, where the prediction of the model for the dual-loop configuration [15] is compared with the experimental results. In this case the first spur is considerably lowered and broadened, and it can be seen that its height is correctly predicted by the model. This suggests that the model predictions for the spurs levels are correct, and thus that the real level of the spurs in the single-loop configuration is around 10 dB higher than what is suggested by Fig. 5.

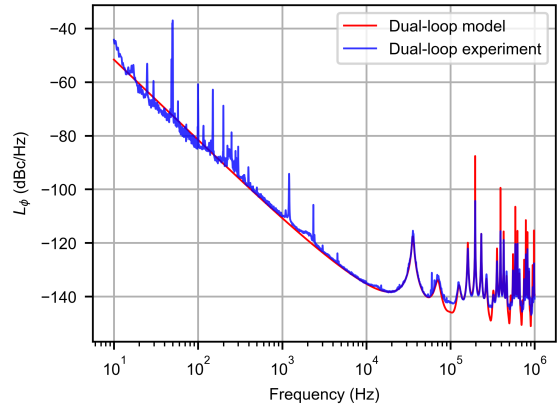


Figure 10: Comparison of the model for the dual-loop configuration with the experimental results. The input noises are the same as in Fig. 9.

III. CONCLUSION AND PERSPECTIVES

The following table summarizes the performances of the different configurations of our system.

Table 1: Phase Noise Comparisons

	Synth 10 GHz	SL 10 GHz	SL 20 GHz	DL 10 GHz	DL 20 GHz
P.N. at 10 KHz (dBc/Hz)	-120	-135	-127	-135	-125
P.N. floor (dBc/Hz)		-140	-132	-140	-132
First spur level (dBc/Hz)		> -72	> -63	-115	-110
E. Power (dBm)	15	15	-5	13	-7

We can compare these figures to some published results. Wishon *et al.*[6] shows typical phase noise levels of -107 dBc/Hz, while displaying the ability to tune the carrier frequency. Sung *et al.*[5] reports a 20 GHz carrier with phase noise of -123 dBc/Hz, using a setup that involves strong injection locking to a master laser. Qi *et al.*[9], using a directly-modulated home-made 1.3 μm laser, obtained a phase noise of -125 dBc/Hz at 10 kHz from the carrier. Considering that the noise floor in [9] is similar to ours, we can ascribe most of the 10 dB phase noise improvement at 10 kHz to the longer resonator length in our setup, as is confirmed by simulations using eq. 1. Concerning standard OEOs with external modulation, phase noises as low as -145 dBc/Hz [15] can be obtained at the cost of a careful optimization of all elements as well as the use of high power lasers (for instance, in [15] a DFB

laser delivering 120 mW was used). The lowest noise reported to date is, to the best of our knowledge, -163 dBc/Hz at 6 kHz offset [14], in a setup using a high power solid-state Nd:YAG laser and a 16 km optical fiber.

In conclusion, we demonstrated the possibility of a stable and powerful oscillation in a DM-OEO both in the single loop and dual loop architectures. We measured a 15 dBm output RF power and a phase noise level of -135 dBc/Hz at 10 kHz from a 10 GHz carrier in both configurations. In the dual-loop configuration, the first spur was as low as -115 dBc/Hz. The system also generates a low-phase noise 20 GHz carrier. The phase noise analysis showed that the laser RIN is the limiting component of the system for frequencies higher than 10 kHz. For better performance one should choose a less noisy laser, which could lead in principle, all other parameters being equal, to an improvement of about 15 dB of the noise floor, for shot-noise-limited operation. In practice the best strategy to improve the performances would be to use a more powerful laser as in [15]. Apart from decreasing the laser RIN, that would also have the added benefit of reducing the need for electrical amplification. With a lower noise floor, a reduction of the fiber loop length may also be acceptable. These results are, to the best of our knowledge, the state-of-the-art of DM-OEOs. This more compact architecture avoiding external modulation is particularly interesting in the perspective of monolithic integration of OEOs in photonic integrated circuits [10]. In this respect, the integration of the delay function is probably the most challenging part. Integrated Si₃N₄ resonators [16] are promising devices for such purpose.

ACKNOWLEDGMENT

We thank O. Llopis from LAAS for providing us with the RF filter, and A. Carré, G. Loas, C. Peucheret and F. Bondu for fruitful discussions.

REFERENCES

- [1] X. S. Yao and L. Maleki, "Optoelectronic microwave oscillator," *Journal of the Optical Society of America B*, vol. 13, no. 8, p. 1725, aug 1996.
- [2] Y. K. Chembo, D. Brunner, M. Jacquot, and L. Larger, "Optoelectronic oscillators with time-delayed feedback," *Reviews of Modern Physics*, vol. 91, no. 3, p. 35006, 2019.
- [3] G. R. Goune Chengui, P. Woafu, and Y. K. Chembo, "The Simplest Laser-Based Optoelectronic Oscillator: An Experimental and Theoretical Study," *Journal of Lightwave Technology*, vol. 34, no. 3, pp. 873–878, 2016.
- [4] G. Giacomelli, M. Calzavara, and F. T. Arecchi, "Instabilities in a semiconductor laser with delayed optoelectronic feedback," *Optics Communications*, vol. 74, no. 1-2, pp. 97–101, dec 1989.
- [5] H. K. Sung, X. Zhao, E. K. Lau, D. Parekh, C. J. Chang-Hasnain, and M. C. Wu, "Optoelectronic oscillators using direct-modulated semiconductor lasers under strong optical injection," *IEEE Journal on Selected Topics in Quantum Electronics*, vol. 15, no. 3, pp. 572–577, 2009.
- [6] M. J. Wishon, D. Choi, T. Niebur, N. Webster, Y. K. Chembo, E. A. Viktorov, D. S. Citrin, and A. Locquet, "Low-noise x-band tunable microwave generator based on a semiconductor laser with feedback," *IEEE Photonics Technology Letters*, vol. 30, no. 18, pp. 1597–1600, 2018.
- [7] A. Thorette, M. Romanelli, S. Bouhier, F. Van Dijk, M. Vallet, and M. Alouini, "Hybrid opto-electronic oscillator for single-sideband microwave photonics," *Electronics Letters*, vol. 54, no. 11, pp. 706–708, may 2018.
- [8] M. L. Liao, J. L. Xiao, Y. Z. Huang, H. Z. Weng, J. Y. Han, Z. X. Xiao, and Y. D. Yang, "Tunable Optoelectronic Oscillator Using a Directly Modulated Microsquare Laser," *IEEE Photonics Technology Letters*, vol. 30, no. 13, pp. 1242–1245, jul 2018.
- [9] B. Qi, H. Wang, B. Zhang, L. Xie, and P. Gong, "Improvement of the phase noise model based on an optoelectronic oscillator using a directly modulated distributed feedback laser," *Optics Communications*, vol. 488, p. 126848, jun 2021.
- [10] P. Primiani, H. Débrégéas, D. Lanteri, M. Alouini, and F. Van Dijk, "Electro-Absorption modulator-based optoelectronic oscillator," in *MWP 2017* -

2017 International Topical Meeting on Microwave Photonics, vol. 2017-December. Institute of Electrical and Electronics Engineers Inc., dec 2017, pp. 1–3.

- [11] E. Rubiola, *Phase noise and frequency stability in oscillators*. Cambridge University Press, jan 2008, vol. 9780521886.
- [12] W. Xu, C. Yang, Z. Wang, and W. Zhao, “Frequency-tripling OEO based on frequency multiplication in saturated electronic amplifier,” *Optik*, vol. 194, oct 2019.
- [13] X. S. Yao, L. Maleki, Y. Ji, G. Lutes, and M. Tu, “Dual-loop opto-electronic oscillator,” in *Proceedings of the Annual IEEE International Frequency Control Symposium*. IEEE, 1998, pp. 545–549.
- [14] D. Eliyahu, D. Seidel, and L. Maleki, “RF amplitude and phase-noise reduction of an optical link and an opto-electronic oscillator,” *IEEE Transactions on Microwave Theory and Techniques*, vol. 56, no. 2, pp. 449–456, 2008.
- [15] O. Lelievre, V. Crozatier, P. Berger, G. Baili, O. Llopis, D. Dolfi, P. Nouchi, F. Goldfarb, F. Bretenaker, L. Morvan, and G. Pillet, “A model for designing ultralow noise single- and dual-loop 10-GHz optoelectronic oscillators,” *Journal of Lightwave Technology*, vol. 35, no. 20, pp. 4366–4374, 2017.
- [16] D. T. Spencer, J. F. Bauters, M. J. Heck, and J. E. Bowers, “Integrated waveguide coupled si_3n_4 resonators in the ultrahigh-q regime,” *Optica*, vol. 1, no. 3, pp. 153–157, 2014.